ACS EARTH AND SPACE CHEMISTRY

Article

Cite This: ACS Earth Space Chem. 2018, 2, 955−967

http://pubs.acs.org/journal/aesccq

Halocarbon Emissions from a Degraded Forested Wetland in Coastal South Carolina Impacted by Sea Level Rise

Yi Jiao,*[,†] Alexander Ruecker,[‡,§] Malte Julian Deventer,[†,∥] Alex T. Chow,[‡] and Robert C. Rhew[†]

[†]Department of Geography and Berkeley Atmospheric Sciences Center, University of California, Berkeley, Berkeley, California 94720, United States

[‡]Biogeochemistry and Environmental Quality Research Group, Clemson University, Georgetown, South Carolina 29440, United States

ABSTRACT: Tropical- and subtropical-storm surges combined with sea level rise cause saltwater intrusions into low-lying coastal ecosystems along the southeastern coast of the United States, gradually converting freshwater forested wetland into saltmarsh. The transition zone between freshwater and saltwater ecosystems becomes a degraded forested wetland, where the combination of high levels of soil organic matter and elevated concentrations of halide ions creates a dynamic biogeochemical environment that may be a potential hotspot for halocarbon formation such as chloroform, methyl chloride, and methyl bromide. This study conducted field measurements at a transition zone in coastal South Carolina to quantify halocarbon exchange rates and laboratory soil incubations to determine the contributions of biotic versus abiotic processes. The degraded forested wetland showed significant chloroform emission rates (146 ± 129 nmol m^{-2} d^{-1}). The degraded forested wetland remained a net sink for methyl chloride and a negligible source/sink for methyl bromide, unlike the saltmarsh which was a significant source for both. The laboratory incubations strongly suggest that methyl halide consumption in soils at the field site was biotic and that production of methyl halides and chloroform was largely abiotic and temperature-dependent, although additional experiments are required to rule out possible biotic production involving heat-resistant microbes. The results suggest that sea level rise and more frequent storm surges derived from global climate change, in the long term, may increase emissions of chloroform from coastal degraded forested wetlands and of methyl halides if salt marshes expand, with potential impacts for stratospheric ozone depletion.

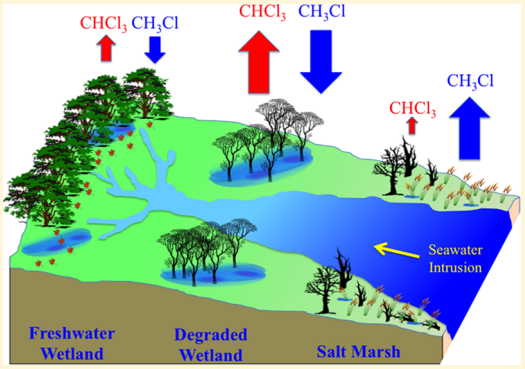

KEYWORDS: *baldcypress-water tupelo swamp, chloroform, methyl chloride, degraded forested wetland, methyl bromide, storm surge*

1. INTRODUCTION

In the lower stratosphere, the photolysis of halocarbons from both anthropogenic and natural sources releases free chlorine and bromine radicals, catalyzing stratospheric ozone depletion. Following the Montreal Protocol in the 1980s, anthropogenic production and use of long-lived ozone-depleting substances (ODSs) have been regulated, and hence since 1997, atmospheric concentrations of these halocarbons have been declining.[1−3] However, noncontrolled halocarbon emissions and emission variations associated with land use change,[4] biomass burning,[5,6] seawater warming,[7,8] and sea level rise[9] could offset some of the reductions achieved by regulatory efforts, highlighting the importance of further exploration of natural sources of ODSs.

Among the natural emitted halocarbons, methyl chloride (CH_3Cl), chloroform ($CHCl_3$), and methyl bromide (CH_3Br) are believed to be the first and second largest natural carrier of reactive chlorine[10,11] and the largest natural carrier of reactive bromine,[12] respectively. However, the known sources presently cannot balance the reported sinks for methyl halides,[3] which suggests that either currently identified sources are underestimated or significant sources are missing. There is also a discrepancy between identified sources and sinks for $CHCl_3$, with sources exceeding sinks by 150−170 Gg each year.[13,14] In order to close the gap in the global budgets of methyl halides and $CHCl_3$, a better mechanistic understanding of natural halogenation reactions and their contribution to the global budgets is needed. In particular, the contribution of abiotic and biotic reaction pathways to the overall halocarbon formations is still a matter of debate.[15−19]

Soils are the second largest natural source for $CHCl_3$ after the ocean,[13,14] and the second largest sink for methyl halides after the reaction with hydroxyl radical ($^{\bullet}OH$).[3] Most studies suggest that $CHCl_3$ formation in soils is mediated by haloperoxidases that oxidize halide ions with H_2O_2, but there is also evidence of abiotic $CHCl_3$ formation in soils,[20] which involves Fenton-like reaction conditions (iron(III) and hydro-

Received: April 9, 2018
Revised: August 1, 2018
Accepted: August 2, 2018
Published: August 2, 2018

DOI: 10.1021/acsearthspacechem.8b00044
ACS Earth Space Chem. 2018, 2, 955−967

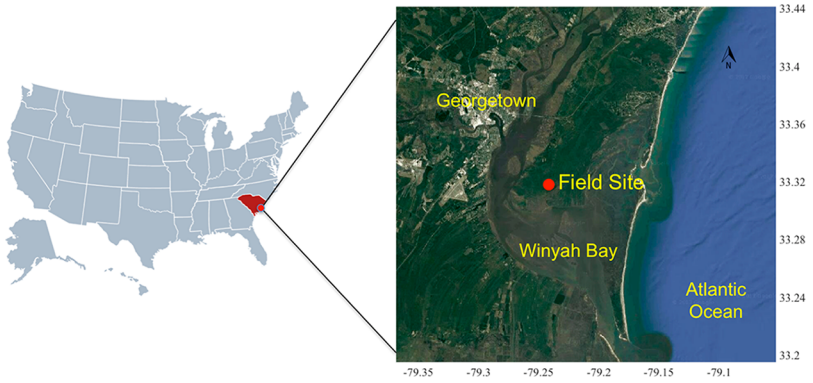

Figure 1. Location of the field site in Northern Inlet-Winyah Bay National Estuarine Research Reserve, South Carolina, U.S.A. The expanded image (Google) shows Winyah Bay and the adjacent Atlantic Ocean with bathymetry. Longitude and latitude coordinates (deg) are labeled.

gen peroxide), elevated halide content, and soil organic matter with resorcin-like dihydroxylated compounds.[18] The biotic pathway of methyl halide formation involves SAM (S-adenosyl-methionine)-dependent methyl transferases that are found widely in plants,[17,21−25] especially those in the Subclass *Dilleniidae*.[26−28] The abiotic formation of methyl halides within soils is believed to be related to Fenton-like reactions with organic matter and halide ions, although different from the mechanisms outlined for chloroform above.[15] The abiotic Fenton-like halogenation reactions are also believed to be responsible for sediment organohalogen formation.[19] Thus, elevated halide content and soil organic matter content can stimulate both the biotic and abiotic pathways of halocarbon production.

Coastal wetlands in southeastern United States that undergo storm-induced seawater intrusion (storm surges) and sea level rise may potentially be hotspots of both $CHCl_3$ and methyl halide production due to their soil biogeochemical properties. Large areas (over 2000 km^2) of low-lying coastal tidal wetlands in the southeastern United States, from Texas to North Carolina, have been slowly inundated with saltwater and will be converted from freshwater forested wetland to degraded forested wetland and ultimately to saltmarsh.[29,30] These degraded forested wetlands, with large amounts of organic matter from fallen branches and leaves and additional halogen input from seawater intrusion, have a significantly different biogeochemical environment in comparison to the adjacent ecosystems. The interaction of halogens with organic-rich sediments can result in the formation of organohalogens,[31,32] thus making the degraded forested wetland potentially a hotspot for halocarbon emissions. However, only one set (n = 4) of chloroform fluxes from this degraded ecosystem have been reported thus far, and the fluxes were on average higher than the bracketing freshwater wetland and saltmarsh ecosystems, an observation that was also consistent with soil core incubations from these same ecosystems.[9] However, the fluxes were also highly variable, leading to questions about the magnitude of annual emissions and the environmental factors controlling these emissions. CH_3Cl and CH_3Br fluxes were also measured,[9] but not yet reported, in the degraded forested wetland, the freshwater wetland, and the saltmarsh ecosystems, providing a basis of comparison for the present study.

In order to evaluate the ozone-depleting impact of the gradual turnover from freshwater forest to saltmarsh over the long-term, and to assess the regional or global implications of the observed biogeochemical transition in coastal ecosystem soils, this study conducted both field and laboratory incubations to quantify spatially and temporally resolved fluxes of $CHCl_3$, CH_3Cl, and CH_3Br. Certain environmental (e.g., temperature, insolation) and biological (e.g., growth cycle of plants, litterfall) controls on fluxes show distinct seasonal cycles, while other potential controls (e.g., flooding, soil salinity, buried soil organic matter) may not. Hence, the seasonality of field-based flux measurements can reveal the relative importance of different biochemical factors and abiotic controls. Furthermore, the production and consumption mechanisms of halocarbons were tested in laboratory soil incubations by manipulating temperature regimes and conducting heat-sterilization on sampled soil cores.

2. EXPERIMENTAL SECTION

2.1. Site Description. Winyah Bay (33°32′N, 79°25′W), a National Estuarine Research Reserve, is located in South Carolina on the southeastern coast of the United States and next to the Atlantic Ocean (Figure 1). The upland freshwater forested wetland is dominated by bald cypress (*Taxodium distictum*) and swamp tupelo (*Nyssa sylvatica* var. *biflora*).[33,34] The coastal wetlands are subject to seawater intrusion due to tropical storm-derived tidal surges in the short term and sea level rise in the long term. The increasing soil salinity has converted coastal freshwater forests to degraded forested wetlands and will eventually convert them to salt marshes.[30,33,35] Forest dieback due to the increasing soil salinity has partially opened the canopy, leaving more ground area exposed to sunlight. The fallen leaves and branches have led to relatively high organic matter content and surged seawater has increased soil salinity.

The Winyah Bay region has a humid subtropical climate, with hot summers (average temperature 32 °C) and mild winters (average temperature 15 °C). Thunderstorms due to hot and humid conditions, together with tropical cyclones or hurricanes, contribute to the annual precipitation of 1427 mm in 2016 (National Weather Service, 2017). In October 2016, Hurricane Matthew traversed the field site and dropped precipitation of up to about 800 mm over a three-day period, submerging the wetland thoroughly for about 2 weeks. Following this flooding period, water levels dropped to subsurface levels in November, exposing the soil to ambient air again.

2.2. In Situ Gas Collections and Measurements. *Static Chamber Description.* In situ static chamber measurements were conducted at a freshwater forested wetland (n = 4),

DOI: 10.1021/acsearthspacechem.8b00044
ACS Earth Space Chem. 2018, 2, 955−967

degraded forested wetland (n = 4) and saltmarsh (n = 4) along a salinity gradient (0.1, 2, and 7 ‰, respectively) on 14−17 May 2012; the freshwater forested wetland and saltmarsh were inundated, and the degraded forested wetland had saturated soil.[9] Subsequently, bimonthly field flux measurements were conducted from January to December 2016 within the degraded forested wetlands. Three replicate sampling sites (within 10 m of each other) were chosen for static chamber measurements in the degraded transition zone undisturbed by human activities. To reduce the potential disturbance to the soils and the microenvironment, open-ended aluminum bases (L × W × H: 52 cm × 52 cm × 15 cm) were inserted into the soil at a depth of about 10 cm in December 2015, one month prior to the first sampling. Fallen and decomposing leaves and branches were enclosed in the chamber footprint.

To conduct the static chamber measurement, an opaque aluminum chamber lid (L × W × H: 53 cm × 53 cm × 45 cm) was placed on top of the previously situated base, which had a 2 cm deep channel filled with deionized water surrounding its lip, to create an airtight seal between base and lid. Two electric fans were mounted inside the chamber to mix the air during the enclosure time period. In four out of the six outings, a transparent chamber lid (same dimensions as the aluminum lid) made of polycarbonate was used to explore the influence of irradiation. To keep temperatures within the chambers stable, the opaque chamber was covered by thermal reflective insulation during sampling while the transparent chamber was actively cooled by pumping water through an aluminum tube (length 13 m, diameter 1 cm) inside the chamber. Chamber air temperatures were recorded every minute with iButton temperature data loggers (Embedded Data Systems, Lawrenceburg, KY); internal temperatures were stable within two degrees Celsius. Blank static chamber measurements using a mirror-polished aluminum sheet with Viton gasket as the base were carried out previously to ensure that the chamber material had no potential contamination in terms of halocarbons.[36]

Sample Collection. Starting from the fifth minute after chamber enclosure, air samples were taken three times at intervals of 15 min into pre-evacuated canisters (1 L, electropolished stainless steel, LabCommerce, Inc., San Jose, CA) for halocarbon analysis and GC headspace vials (10 mL, glass) for the greenhouse gases (CO_2, CH_4) analysis, respectively. When taking the air samples, a stainless steel vent tube was opened to ambient air to maintain pressure equilibrium and avoid drawing air from the soil pore space.

Sample Measurements. Each gas sample was measured at least twice for halocarbons and greenhouse-gas concentrations. For halocarbon ($CHCl_3$, CH_3Cl and CH_3Br) analysis, samples were preconcentrated with cryo-trap and then analyzed by gas chromatography coupled with a mass spectrometer (GC/MS; Agilent 6890*N*/5973, Agilent Technologies, Santa Clara, CA).[37] Calibration curves were constructed before and after each batch of samples with a natural air standard collected at Trinidad Head, CA, which was calibrated at the Scripps Institution of Oceanography, University of California at San Diego. For CO_2 and CH_4 analyses, samples were analyzed as duplicates using a Shimadzu GC2014 greenhouse-gas analyzer coupled with three detectors: ECD/FID/TCD. Certified greenhouse-gas standard mixtures (Air Liquide LLC., Houston, TX) were used for calibration of CO_2 and CH_4. The concentrations were reported in parts per million (ppm) for greenhouse gases and parts per trillion (ppt) for halocarbons.

Flux Calculation. Positive fluxes (emissions) were calculated on the basis of the slope derived from the best linear fit between the corresponding gas concentrations and enclosure time. When negative fluxes (uptakes) were observed, a first-order consumption rate (k) was calculated and then normalized to Northern Hemisphere background air concentrations (7.53 ppt, 542.2 ppt, 6.95 ppt for $CHCl_3$, CH_3Cl, and CH_3Br respectively as of 2012[3]). Fluxes were reported as the change of the number of moles of gas per unit area and per unit time (moles m^{-2} d^{-1}). Flux errors were derived from the propagation of the 90% confidence interval of the slope and in the number of moles of air within the chambers. The paired-t-test (type I error rate at 5% level) was applied to detect statistically significant differences between fluxes measured with opaque and transparent chambers.

Soil Property Measurements. Surface soil (0−5 cm) samples were collected using a small spade and transported to the laboratory for further analysis. Dissolved organic carbon (DOC) and total dissolved nitrogen (TDN) of soil extracts were analyzed with at least two replicate extracts from each site. The soil extract was prepared and analyzed according to Emmerich et al.[38] and Ruecker et al.[39] Gravimetric soil moisture ($g_{H_2O}/g_{soil\ wet\ wt.}$) was measured by water loss after oven-drying subsamples (50 g, fresh weight) at 105 °C overnight (except for January and December). Soil temperatures (at ∼3 cm depth) were recorded with iButton temperature data loggers (Embedded Data Systems, Lawrenceburg, KY). Soil pH measured previously in this ecosystem was 7.0.[9]

2.3. Laboratory Soil Core Incubations. *Soil Collection and Incubation.* Intact soil cores (n = 10, depth: 5.0 cm, diameter: 4.5 cm) from the degraded forested wetland were collected on July 28 and 29, 2016 using a slide hammer (AMS, Inc., American Falls, ID) and stored at 5 °C until the start of experiments. Soil cores inside a sheath and base (stainless steel or aluminum) were placed in 1.9 L Mason jars for incubations. The jar was initially sealed and 50−100 mL of headspace was withdrawn to remove accumulated gas within the soil pores. Then the jars were opened and flushed with ambient air for approximately 30 s prior to sealing again with a Viton O-ring and a stainless steel lid to start the actual incubation. A short length of stainless steel tubing was used both as a sampling volume and as the conduit between the jar and the preconcentration system of the GC/MS. Approximately 15 mL of air sample was drawn from the jar headspace every 40 min for three times, starting at 1 min after sealing. The gas fluxes were calculated on the basis of the change of the number of moles of gas species per unit time and per unit exposed soil core surface area (15.9 cm^2), reported in units of moles m^{-2} d^{-1}. After the first incubation, a standard was measured. Meanwhile, the jar was opened and flushed with ambient air. The soil cores were then measured a second time within an hour of the first incubation.

Temperature-Controlled Incubation. The same batch of soil cores were incubated at different temperatures, ranging from 5 to 40 °C, at steps of 5 °C. To simulate different temperatures, Mason jars were situated in a temperature controlled water/ethylene glycol bath (Model 1180S, VWR International, West Chester, PA). At each temperature, the jars were sealed first and then placed in the bath for at least 12 h in order to reach an equilibrium temperature with the surrounding liquid bath. Water loss in between runs was

DOI: 10.1021/acsearthspacechem.8b00044
ACS Earth Space Chem. 2018, 2, 955−967

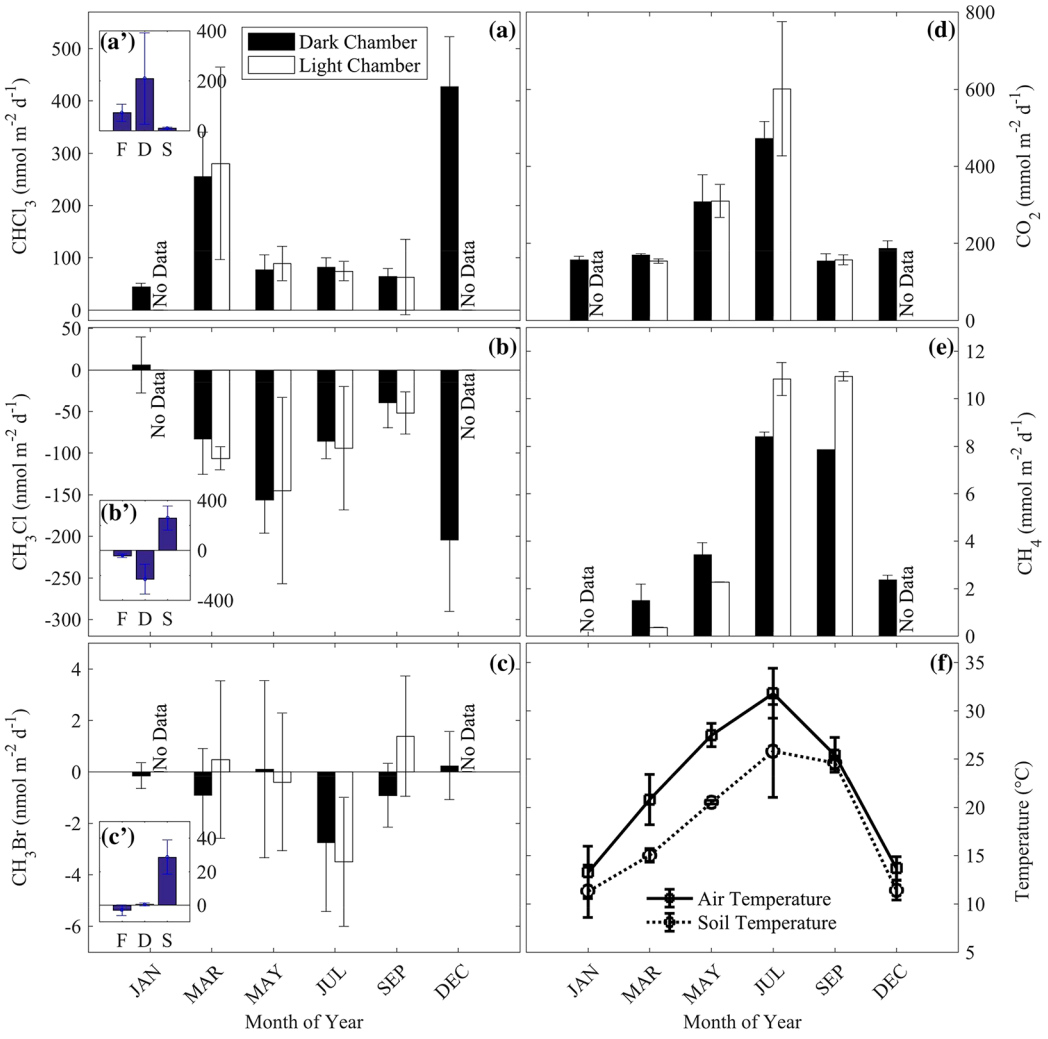

Figure 2. Bimonthly fluxes in 2016 from the degraded forested wetland (a) chloroform ($CHCl_3$), (b) methyl chloride (CH_3Cl), (c) methyl bromide (CH_3Br), (d) carbon dioxide (CO_2), (e) methane (CH_4), and (f) annual air/soil temperatures. Inset bar plot of fluxes in May 2012, of (a') chloroform ($CHCl_3$),[9] (b') methyl chloride (CH_3Cl), (c') methyl bromide (CH_3Br) from freshwater forested wetland (F), degraded forested wetland (D), and saltmarsh (S) along a salinity gradient. "No Data" indicates the corresponding measurement was not taken. Height of the bars represent the averaged values of measured fluxes among replicates (n = 3 for a,b,c,d and e; n = 2 for f ; n = 4 for a', b', and c'), and error bars represent the standard deviations of measured fluxes among replicates.

assumed to be negligible. Prior to each incubation, the jar was flushed with ambient air for 30 s, and gas fluxes were quantified as described above.

Thermal Sterilization. To distinguish between abiotic and biotic contributions to halocarbon emissions, aluminum-foil-covered soil cores were thermally sterilized at 150 °C at atmospheric pressure for 2 h to destroy the enzymes and stop microbial activity in the soil.[15,40] The soils were not heated to complete dryness and deionized water was added to the soil to account for water loss during the thermal sterilization process. Approximately 12 h later, the sterilized soil cores were incubated for flux measurements as described above, along the same temperature gradient (range: 5 to 40 °C with steps of 5 °C). Paired-*t*-test (type I error rate at 5% level) was applied on flux comparisons between soil cores before and after thermal treatments.

Arrhenius Formula. The effect of temperature on halocarbon production was explored by fitting measured fluxes from the temperature-controlled incubations with the Arrhenius equation. The Arrhenius formula, proposed by Svante Arrhenius in 1889, is usually used for the temperature dependence of reaction rates:

$$k = Ae^{-E_a/RT} \quad (1)$$

where A is the frequency factor or pre-exponential factor, T is the soil temperature in Kelvin, k is the reaction rate constant (here k represents trace gas fluxes in nmol m^{-2} d^{-1}), E_a is the activation energy for the reaction (J mol^{-1}), and R is the universal gas constant (8.314 J mol^{-1} K^{-1}). The linear relationship between temperature and reaction rate constant is shown by rearranging the Arrhenius equation as follows:

$$\ln(k) = -\frac{E_a}{R}\cdot\frac{1}{T} + \ln(A) \quad (2)$$

With the temperature gradient incubations of the soil cores (range: 5 to 40 °C with steps of 5 °C), the logarithmic value of chloroform fluxes was plotted against the inverse of temperature (in Kelvin).

DOI: 10.1021/acsearthspacechem.8b00044
ACS Earth Space Chem. 2018, 2, 955−967

Table 1. Temperatures and Soil Chemical Properties at the Field Sampling Sites (n = 3)[a]

date	air temp (°C)	soil temp (°C)	soil moist. (H_2O wt/wet wt, %)	DOC (mg/L)	TDN (mg/L)
01/27/2016	13.2 ± 2.7	11.3 ± 2.7	*	*	*
03/24/2016	20.8 ± 2.6	15.0 ± 0.7	25.7 ± 5.2	*	*
05/26/2016	27.5 ± 1.2	20.5 ± 0.2	14.0 ± 1.1	11.8	0.5
07/28/2016	31.8 ± 2.6	25.8 ± 4.8	7.5 ± 2.8	11.6	1.1
09/26/2016	25.4 ± 1.8	24.6 ± 0.7	50.5 ± 3.2	14.4	0.8
12/05/2016	13.7 ± 1.2	11.4 ± 1.0	*	16.6	1.8

[a]Symbol (*) indicates that the corresponding measurement was not taken.

Table 2. Chloroform ($CHCl_3$) Fluxes from Coastal Ecosystems (Freshwater Forested Wetland, Degraded Forested Wetland and Salt Marsh) along a Salinity Gradient in South Carolina

		$CHCl_3$ flux (nmol m^{-2} d^{-1})		
study	note	freshwater forested wetland	degraded forested wetland	salt marsh
Wang et al. (2016)[9]	one-time measurement	71.9 ± 33.4	209 ± 183	9.7 ± 3.9
this study	annual mean	--	146 ± 129	--
	maximum	--	511 ± 19	--

3. RESULTS

3.1. Seasonal Variabilities of Halocarbons ($CHCl_3$, CH_3Cl, and CH_3Br) Fluxes from Degraded Forested Wetland. *3.1.1. Chloroform ($CHCl_3$).* The degraded forested wetland was consistently a net source for $CHCl_3$ over the period of measurement, with an overall annual mean net flux of 146 ± 129 nmol m^{-2} d^{-1} and a full range of 12−511 nmol m^{-2} d^{-1} (Figure 2a). These fluxes showed large temporal variability, with the highest fluxes observed in December 2016 (427 ± 95 nmol m^{-2} d^{-1}) and the lowest fluxes observed in January 2016 (44 ± 7 nmol m^{-2} d^{-1}). The three study sites also showed large spatial variability, illustrated by the standard deviations. However, spatial variability was significantly smaller than variability over time (two-way analysis of variance at p = 0.05). Variations in the seasonal $CHCl_3$ pattern did not resemble the seasonal variations of air or soil temperature, suggesting that temperature was not the major controlling factor for $CHCl_3$ emissions between the sites. Differences between the opaque and the transparent chamber were found to be statistically not significant (paired-t-test). Environmental parameters other than temperature, solar radiation, and soil moisture were not concurrently monitored and are excluded from the discussion. Average $CHCl_3$ fluxes from 2016 accounted for 69.9% of those measured in May 2012, but the range of fluxes from both studies were comparable.[9]

3.1.2. Methyl Chloride (CH_3Cl). The degraded forested wetland was a net sink for CH_3Cl (Figure 2b). Negative fluxes were observed at nearly all sampling spots in 2016, with an annual mean net flux of −90 ± 61 nmol m^{-2} d^{-1} and a range of −293−41 nmol m^{-2} d^{-1}. Large temporal variability was observed, with the largest uptake rate of CH_3Cl in December with −204 ± 86 nmol m^{-2} d^{-1}. In January, the soil showed negligible average CH_3Cl fluxes (6 ± 34 nmol m^{-2} d^{-1}). The bimonthly fluxes of CH_3Cl were also highly variable over time and did not follow the annual temperature pattern. No statistically significant difference (paired-t-test) was observed between CH_3Cl fluxes measured with the opaque chamber and the transparent chamber. In May 2012, the degraded forested wetland was a large net CH_3Cl sink (−232 ± 120 nmol m^{-2} d^{-1}), in contrast to the small net uptake rates observed at the freshwater forested wetland (−44 ± 15 nmol m^{-2} d^{-1}) and the relatively large net emissions observed at the saltmarsh (258 ± 95 nmol m^{-2} d^{-1}) (Figure 2b').

3.1.3. Methyl Bromide (CH_3Br). In contrast to $CHCl_3$ which showed only emissions and to CH_3Cl which primarily showed uptake, no significant exchange rate was observed for CH_3Br from the degraded forested wetland (Figure 2c). Bimonthly measured net fluxes fluctuated between slightly positive and slightly negative values in the range of −6 nmol m^{-2} d^{-1} to 4 nmol m^{-2} d^{-1} with an annual mean flux of −3.1 ± 2.6 nmol m^{-2} d^{-1}. The temporal variability also did not follow soil or air temperature trends. In the 2012 study (Figure 2c'), the degraded forested wetland also showed negligible fluxes (0.3 ± 0.8 nmol m^{-2} d^{-1}), whereas the saltmarsh was a source (28.6 ± 10.2 nmol m^{-2} d^{-1}) and freshwater forested wetland a modest sink (−3.1 ± 3.2 nmol m^{-2} d^{-1}).

3.1.4. Methane (CH_4) and Carbon Dioxide (CO_2). The degraded forested wetland soil was a net source for both CO_2 and CH_4. The annual CO_2 emission rates were 267 ± 157 mmol m^{-2} d^{-1} and the annual CH_4 emission rates were 5.3 ± 4.2 mmol m^{-2} d^{-1} (Figure 2d,e). The annual emission patterns of both CO_2 and CH_4 followed the seasonal pattern in ambient/soil temperatures, which suggested that the production of CO_2 and CH_4 were primarily mediated by temperature-dependent microbial activity (Tables 1 and 2).

3.2. Lab Soil Incubations for Halocarbons ($CHCl_3$, CH_3Cl, and CH_3Br) Fluxes. *3.2.1. Soil Laboratory Incubation Fluxes in Comparison to Field Measurements.* The laboratory soil core incubation results yielded similar results to the field measurements from July, when the soil cores were collected. Both soil incubations and field measurements demonstrated that the degraded forested wetland soils emitted a significant amount of $CHCl_3$. The soil cores incubated at room temperature (T = 21.5 °C, n = 8) revealed a mean flux of 39 ± 17 nmol m^{-2} d^{-1}, which was lower than but of the same magnitude as the field measurements in July (opaque and transparent chambers averaged, 78 ± 18 nmol m^{-2} d^{-1}). Soil core incubations also showed the same magnitude and direction of CH_3Cl exchange rate (−61 ± 34 nmol m^{-2} d^{-1}) and CH_3Br fluxes (−2.2 ± 0.8 nmol m^{-2} d^{-1}) as in the field in July (CH_3Cl flux: −90 ± 48 nmol m^{-2} d^{-1}, CH_3Br flux: −2.2 ± 0.1 nmol m^{-2} d^{-1}, opaque and transparent chambers averaged).

3.2.2. Soil Core Fluxes after Thermal Treatments. The fluxes observed from the untreated room temperature soil cores, described above, were compared with room temperature

DOI: 10.1021/acsearthspacechem.8b00044
ACS Earth Space Chem. 2018, 2, 955−967

(T = 21.5 °C) flux measurements of the same soil cores following thermal sterilization and restoration of soil moisture levels. The thermal treatment was designed to stop enzymatic and microbial activity during a short heating period that limited the physical disturbance to the soil structure. Mean $CHCl_3$ fluxes slightly increased from pretreament values of 39 ± 17 nmol m^{-2} d^{-1} (n = 4, see above) to 47 ± 41 nmol m^{-2} d^{-1} (n = 2) post-treatment (Figure 3a). However, differences

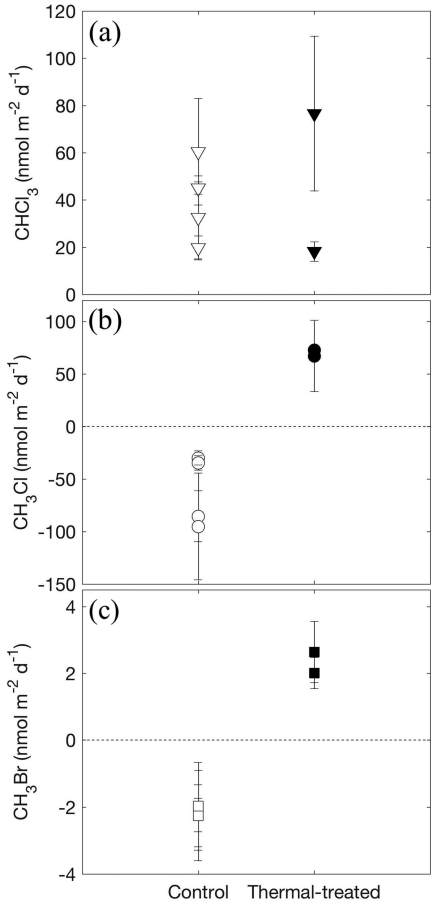

Figure 3. Plot of (a) chloroform ($CHCl_3$), (b) methyl chloride (CH_3Cl), and (c) methyl bromide (CH_3Br) fluxes from soil cores pre- (n = 4) and post-thermal treatment (n = 2). The incubations were conducted at room temperature (22 °C). Values above the dashed line at zero indicate a net source, whereas values below the dashed line indicate a net sink. Error bars represent the standard deviation of the replicates.

were statistically not significant (paired-t-test). In contrast, after thermal treatment soils acted as sources of CH_3Cl and CH_3Br uniformly, whereas they acted as net sinks before heat treatment. The methyl halide fluxes switched from pretreatment net sinks (see above) to post-treatment sources of CH_3Cl (70 ± 4 nmol m^{-2} d^{-1}) and CH_3Br (2.3 ± 0.4 nmol m^{-2} d^{-1}) (Figure 3).

3.2.3. Temperature Gradient Incubations. $CHCl_3$ fluxes from both pre- and post-thermal treated soil cores increased with incubation temperatures (Figure 4a). Arrhenius plots of the natural log of $CHCl_3$ emission fluxes versus $1/T$ showed similar slopes and correlations for the pretreated (R^2 = 0.96) and post-thermal treated soil incubations (R^2 = 0.93, Figure 4d).

Prethermal treated soil cores gradually switched from CH_3Cl sinks to sources as temperature increased: −180 to −240 nmol m^{-2} d^{-1} at 5−15 °C, −15 to −60 nmol m^{-2} d^{-1} at 20−25 °C, 50−130 nmol m^{-2} d^{-1} at 30−35 °C and 320 nmol m^{-2} d^{-1} at 40 °C (Figure 4b). For individual flux measurements, the largest uptake of CH_3Cl was observed at the lowest temperature (−314 ± 73 nmol m^{-2} d^{-1} at 5 °C), and the largest emission was observed at the highest temperature (381 ± 110 nmol m^{-2} d^{-1} at 40 °C). However, post-thermal treated soil cores became CH_3Cl sources uniformly under all temperatures. CH_3Cl fluxes from post-thermal treated soil cores also increased with incubation temperature and can be represented by the Arrhenius equation (R^2 = 0.89, Figure 4e, eq 2). Plotting the Arrhenius relation for methyl halides from prethermal treated soil cores is not possible because of negative methyl halide fluxes.

Soil core incubations revealed negligible CH_3Br absorption rates and emission rates before and after the thermal treatments, respectively (Figure 4c), which is consistent with the field results. Control soil cores were CH_3Br sinks at any temperature uniformly but switched to CH_3Br sources after the thermal treatment. The Arrhenius fit showed a linear trend with a moderate R^2 value (R^2 = 0.405, Figure 4f).

4. DISCUSSION

4.1. Chloroform ($CHCl_3$). *4.1.1. Comparison to Fluxes from Other Ecosystems.* Results suggest that the transitional zone (degraded forested wetland) of coastal South Carolina can be a significant source of $CHCl_3$ to the atmosphere. The mean ±1σ annual $CHCl_3$ flux calculated from the bimonthly measurements is 146 ± 129 nmol m^{-2} d^{-1} from the field chambers and 39 ± 17 nmol m^{-2} d^{-1} from laboratory incubations. These emission rates are slightly lower than but comparable to the 209 ± 183 nmol m^{-2} d^{-1} emissions observed at this site on May 12−14, 2012.[9] Nevertheless, the mean (146 nmol m^{-2} d^{-1}) and the highest (511 nmol m^{-2} d^{-1}) of observed net $CHCl_3$ emission rates in 2016 are larger than or comparable to reported fluxes from other natural significant $CHCl_3$ sources (Table 3), including tropical rainforest,[41] subtropical shrubland and saltmarsh,[9,42] temperate peatland,[43] temperate coniferous forest,[44] temperate pasture,[45] temperate saltmarsh,[45] rice field,[41,46,45] boreal pine forest,[48] subarctic shrubland, wetland, bog, birch forest and coniferous forest,[49] and arctic tundra.[11] Similar to most of these ecosystems, $CHCl_3$ fluxes observed here show relatively high spatial variability, despite the proximity of sampling sites and visible homogeneity of enclosed soils. Given the experience at other ecosystems,[44,50] it is unlikely that these measurements captured the full spatial variability of fluxes.

It is possible that increased availability of Cl^- associated with storm surges contributes to the high $CHCl_3$ fluxes in the degraded forested wetland, the spatial extent of which are expected to increase with projected sea level rise. The May 2012 study[9] also showed that $CHCl_3$ emissions in the degraded forested wetland was greater than those in the adjacent saltmarsh and freshwater forested wetland (Figure 2a,a', Table 2), although the freshwater wetland was flooded at that time. Demonstrating the enhancement of $CHCl_3$ emissions from the salt-induced degradation of freshwater forested wetlands will require a corresponding study in unaltered freshwater forested wetlands. The consistently smaller $CHCl_3$ emissions from saltmarsh sites both here as

DOI: 10.1021/acsearthspacechem.8b00044
ACS Earth Space Chem. 2018, 2, 955−967

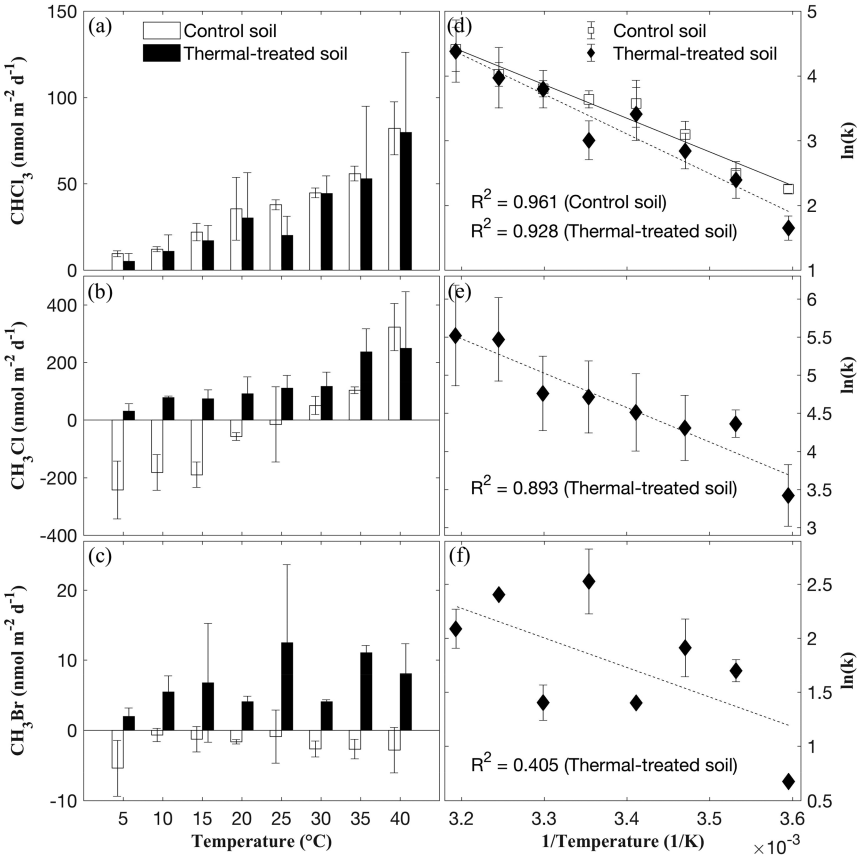

Figure 4. Bar plot of (a) chloroform ($CHCl_3$), (b) methyl chloride (CH_3Cl), and (c) methyl bromide (CH_3Br) fluxes in laboratory soil incubations (n = 4) at different temperatures. Arrhenius plots of production rates of (d) chloroform ($CHCl_3$), (e) methyl chloride (CH_3Cl), and (f) methyl bromide (CH_3Br) from incubated soil cores (n = 4) at different temperatures. k represents the emission rate of the corresponding halocarbons (unit: nmol m^{-2} d^{-1}). Error bars represent the standard deviation of measured fluxes among replicates.

well as elsewhere[42,45] suggests that salt marshes are indeed smaller sources of $CHCl_3$.

4.1.2. Abiotic versus Biotic Mechanisms of $CHCl_3$ Production. Both biotic and abiotic mechanisms that produce $CHCl_3$ are known, and assessing which mode of production dominates in the degraded forested wetland is necessary to predict changes in future emissions. Regarding biotic mechanisms, haloperoxidases are known to catalyze the halogenation reaction among hydrogen peroxide, organic matter, and halide ion (X: Cl^-, Br^-, I^-) resulting in the production of relevant intermediate compounds including HOX or enzyme-bound intermediates, which then contribute to the formation of haloform.[52−56] Hoekstra et al.[57] conducted laboratory-based simulating reactions with humic acid, chloride, and chloroperoxidase and also suggested that chloroperoxidase-mediated chlorination of humic materials is an environmentally significant process accounting for $CHCl_3$ emissions from natural soils. Field measurements also showed that wood-degrading areas and soils with a humic layer could emit more $CHCl_3$ (maximum 201.0 nmol m^{-2} d^{-1}) than areas without humic layers.[58]

However, the activity of chloroperoxidases, like most enzymes, is inhibited at high temperatures. For example, the activity of chloroperoxidase from the fungus *Caldariomyces fumago* reaches 100% at 35 °C and drops to almost 0% after incubation at 60 °C for 15 min.[59] Another study showed that chloroperoxidase from the same fungus retained only about 10% peroxidase activity after exposure at 50 °C for 6 h.[60] Much higher thermostability (activity midpoint temperature of 90 °C) was observed from a different fungus chloroperoxidase (*Curvularia inaequalis*), but its activity reduced to 0% at 100 °C.[61] The loss of activity presumably represents the denaturing of the enzyme. In the controlled incubations with soil cores pre- and post-thermal treatment, no significant difference was observed in terms of $CHCl_3$ fluxes (paired-t-test, n = 4). Assuming that chloroperoxidase was destroyed during the thermal treatment process (2 h at 150 °C), these results suggest that abiotic production dominates the $CHCl_3$ emissions at the field site. The linear Arrhenius relation with high R^2 values over the whole temperature range is consistent with a nonenzymatic process (Figure 4d), unless the dominant chloroperoxidase has high thermostability. One caveat is that the thermal treatment may decrease organic matter content in soils and increase dissolved organic matter content in pore water,[62] which may change concentrations of available reactants involved in the abiotic production of halocarbons.

The behavior of production in the degraded forested wetland may differ from other forest soils. For example, Danish spruce forest soil has peak $CHCl_3$ emissions in warm and humid spring and autumn, thus suggesting that soil microorganisms were responsible for the $CHCl_3$ production.[63] However, at our field sites, the peak $CHCl_3$ emissions were observed in December, during the coldest period of the year with relatively low CO_2 emission rates (Figure 2d). The different phase of CO_2 and $CHCl_3$ fluxes suggests that $CHCl_3$ emissions do not correspond with the general activity of

DOI: 10.1021/acsearthspacechem.8b00044
ACS Earth Space Chem. 2018, 2, 955−967

Table 3. Literature Summary of Chloroform ($CHCl_3$) Emission Rates at Different Ecosystems

geographic zone	ecosystem	$CHCl_3$ flux range (mean)[b] (nmol m^{-2} d^{-1})	n	location	time of measurement	ref
tropical	rainforest soil	(25)	6	2°S 50°W	1987 (May)	41
tropical	rice paddies	(201)	--	23°09′N 113°21′E	1995 (Aug-Oct)	46
subtropical	rice paddies	20−101	21	30°N 104°E	1985−1987	41
subtropical	agricultural soil (canola, crops)	34−50	3	29°30′N 106°42′E	1988 (Apr)	41
subtropical	shrubland	−3−31 (6.6)	41	32−33°N 116−117°W	1997−2000	42
subtropical	salt marsh	−1−83 (15)	32	32°N 117°W	1997−2000	42
subtropical	degraded forested wetland	12−511 (146 ± 129)	36	33°32′N 79°25′W	2016 (bimonthly)	c
subtropical	degraded forested wetland[a]	20−60 (39 ± 17)	8	33°32′N 79°25′W	2016 (Jul)	c
subtropical	degraded forested wetland	(209 ± 183)	4	33°16′N 79°14′W	2012 (May)	9
subtropical	salt marsh	(10 ± 4)	4	33°16′N 79°14′W	2012 (May)	9
subtropical	freshwater forested wetland	(72 ± 33)	4	33°16′N 79°14′W	2012 (May)	9
temperate	rice paddies	0−300	12	38°06′N 121°39′W	2009 (life cycle)	47
temperate	rice paddies	121−885	--	40°30′N 116°24′E	1992−1993 (Jul-early Oct)	46
temperate	forest soil	25−435	56	38°S 146°W	1985 (Apr-Nov)	41
temperate	tussock grassland	9−965 (362 ± 322)	10	40°41′S 144°41′E	1999−2001 (quasi-annual)	45
temperate	pasture	14−422 (241 ± 221)	10	40°41′S 144°41′E	1999−2001 (quasi-annual)	45
temperate	eucalypt forest soil/litter	322−1005 (603 ± 583)	8	40°41′S 144°41′E	2000−2001 (quasi-annual)	45
temperate	melaleuca forest soil/litter	32−191 (64 ± 60)	10	40°41′S 144°41′E	2000−2001 (quasi-annual)	45
temperate	wetland (saltmarsh)	3−54 (15 ± 9)	10	40°41′S 144°41′E	2000−2001 (quasi-annual)	45
temperate	rain forest (fir, hemlock)	−26−125	12	49°52′N 125°20′W	2012 (May)	50
temperate	peatland (coniferous forest)	25−4574 (3352)	14	53°20′N 9°49′W	1998 (Sep)	43
temperate	[eatland (bog)	2−652	22	53°20′N 9°49′W	1998 (Sep)	43
temperate	peatland soil (drained)[a]	3−3004 (258 ± 288)	36	38°06′N 121°39′W	2009−2010 (monthly)	51
temperate	coastal marsh	34−101 (78)	26	53°19′N 9°54′W	1998 (Sep)	43
temperate	inland marsh	117−262	10	53°20′N 9°49′W	1998 (Sep)	43
temperate	coniferous forest soil	3−402	20	56°23′N 8°57′E	2009 (Mar, Jun)	44
temperate	coniferous forest soil	8−538	30	56°02′N 12°04′E	2009 (Mar, Jun, Sep)	44
subarctic	coniferous forest soil	8−573	20	68°13′N 19°42′E	2012−2014 (spr, sum, aut)	49
subarctic	birch forest soil	2−116	20	68°13′N 18°49′E	2012−2014 (spr, sum, aut)	49
subarctic	boreal pine forest	0−241 (20−160)	16	61°51′N 24°17′W	2005 (Apr, May, Jun)	48
subarctic	lichen-graminoid heath	3−27	10	61°11′N 45°22′W	2012−2014 (spr, sum, aut)	49
subarctic	bog	2−26	20	68°26′N 18°34′E	2012−2014 (spr, sum, aut)	49
subarctic	shrubland (birch/willow)	1−8	18	61°09′N 45°21′W	2012−2014 (spr, sum, aut)	49
arctic	sedge wetland	10−105	10	66°59′N 50°54′W	2012−2014 (spr, sum, aut)	49
arctic	mossy tundra	(293)	2	68°N 50°W	1986 (Jul)	41
arctic	tundra (dwarf-shrub)	3−35	50	67°N 50°W 69°N 53°W	2012−2014 (spr, sum, aut)	49
arctic	tundra	0−118 (36.1)	16	68°N 149°W	2006 (Aug)	11
arctic	tundra	1.3−258 (47.5)	60	71°N 157°W	2005 (Jun., Aug.), 2006 (Jul.)	11

[a]Denotes soil core incubations, all the others are static chamber measurements. [b]When available, the standard deviation is reported. [c]Denotes this study.

microorganisms or fungi, assuming that CO_2 is largely a function of their respiration. Albers et al.[44] studied coniferous forests soil and reached a similar conclusion that the general microbial activity could not explain the $CHCl_3$ production within soils.

Several abiotic $CHCl_3$ production mechanisms in soil have been proposed. One abiotic mechanism is the decarboxylation of trichloroacetic acid (CCl_3COOH).[64−67] Trichloroacetic acid in the soil could arise from multiple pathways, including the oxidative biotransformation of trichloroethene (C_2HCl_3) and tetrachloroethene (C_2Cl_4)[68] and mainly anthropogenic use of herbicide.[69] The addition of trichloroacetic acid into spruce forest soil leads to an increased release of $CHCl_3$, suggesting that trichloroacetic acid does contribute to the $CHCl_3$ formation.[70] However, the field site is located at remote coastal forested area, far away from industrial pollution sources, and the $CHCl_3$ fluxes showed large temporal variations, suggesting that decarboxylation alone is not likely to explain the high $CHCl_3$ fluxes from soil.

Another possible abiotic mechanism for $CHCl_3$ production involves the transformation of carbon tetrachloride (CCl_4) in iron(III)-reducing environments through mineral mediated or sulfate-reducing reactions.[71−73] The measured CCl_4 fluxes were uniformly negligible (0.4 ± 2.1 nmol m^{-2} d^{-1}) and showed no correlations to $CHCl_3$ fluxes in this study, suggesting that the pathway of CCl_4 transformation could not account for the $CHCl_3$ production at the field sites. Huber et al.[18] conducted laboratory incubations and concluded that Fenton-like reaction conditions (iron(III) and hydrogen peroxide), elevated halide content, and an extended reaction time could produce $CHCl_3$ through the degradation pathway starting from resorcin-like dihydroxylated compounds. Breider

DOI: 10.1021/acsearthspacechem.8b00044
ACS Earth Space Chem. 2018, 2, 955−967

Table 4. Literature Summary of Methyl Chloride (CH_3Cl) Consumption Rates at Different Ecosystems

geographic zone	ecosystem	CH_3Cl consumption rate (nmol m^{-2} d^{-1})[b]	n	location	time of measurement	ref
tropical	rainforest soil	(129.5)	8	2°S 50°W	1985 (Jul)	41
tropical	rainforest soil	(176.6)	6	2°S 50°W	1987 (May)	41
subtropical	degraded forested wetland	−41−292 (90 ± 61)	36	33°16′N 79°14′W	2016 (bimonthly)	c
subtropical	degraded forested wetland[a]	25−131 (61 ± 34)	8	33°16′N 79°14′W	2016 (Jul)	c
subtropical	shrubland (coastal)	6−250	10	32°52′N 117°15′W	1997 (Dec), 1998 (Mar, Jul), 2000 (May)	78
subtropical	shrubland (chaparral)	46−430	10	32°52′N 117°14′W	1998 (Apr), 2000 (May)	78
subtropical	shrubland (desert)	4.4−133	6	33°38′N 116°22′W	1998 (Jan), 2000 (Apr)	78
temperate	tussock grassland	−87−480 (144 ± 161)	10	40°41′S 144°41′E	1999−2001 (quasi-annual)	45
temperate	pasture	4−310 (144 ± 119)	10	40°41′S 144°41′E	1999−2001 (quasi-annual)	45
temperate	eucalypt forest soil/litter	−367−310 (51 ± 184)	8	40°41′S 144°41′E	2000−2001 (quasi-annual)	45
temperate	melaleuca forest soil/litter	37−480 (283 ± 311)	10	40°41′S 144°41′E	2000−2001 (quasi-annual)	45
temperate	wetland (saltmarsh)	−215−10 (−85 ± 90)	10	40°41′S 144°41′E	2000−2001 (quasi-annual)	45
subarctic	boreal forest soil	(400 ± 150)[b]	6	60−64°N 147−150°W	2002 (Sep, Oct)	40
arctic	greenland mossy/gras	47−94	12	68°N 50°W	1986 (Jul)	41
arctic	coastal tundra (drained)	(617 ± 43)	9	71°N 157°W	2005 (Jun, Aug)	37
arctic	coastal tundra (moist)	(483 ± 77)	8	71°N 157°W	2005 (Jun, Aug)	37
arctic	coastal tundra (wet)	(195 ± 57)	10	71°N 157°W	2005 (Jun, Aug)	37
arctic	coastal tundra (flooded)	(14 ± 4)	12	71°N 157°W	2005 (Jun, Aug)	37

[a]Denotes soil core incubations, all the others are static chamber measurements. [b]The flux format is a range (mean or mean ± standard deviation), and it is the consumption rate (positive values represent absorption from the air, negative values represent emission from the soil). [c]Denotes this study.

et al.[74] also simulated $CHCl_3$ formation with pure chemicals (phenol and propanone) in laboratory incubations. This abiotic pathway could happen in soil with a typical pH range of 4.5−7.5[75] and could potentially explain the high $CHCl_3$ emission features because the field site meets two of the essential factors: high organic matter content and elevated soil salinity.

In this study, the highest $CHCl_3$ flux was observed in December, after the water level retreated back to subsurface levels after Hurricane Matthew. Page et al.[76] found that reactive oxygen species, including hydroxyl radical (·OH), intermediacy of hydrogen peroxide (H_2O_2), were produced during the oxidation of humic acid in soils by exogenous O_2. Thus, one hypothesis is that the Hurricane Matthew-induced water level rise could have produced an environment conducive to iron reduction to Fe (II), which could then participate in Fenton reactions once H_2O_2 becomes available when water levels drop. In this case, the soil redox potential may relate to $CHCl_3$ formation. Using CH_4 flux as an indicator for soil redox potential, the fact that relatively low CH_4 fluxes were measured in spring and winter when high $CHCl_3$ fluxes were observed (Figure 2a,e) suggests that $CHCl_3$ production favorably occurs when the system is not anaerobic.

Although the $CHCl_3$ production mechanism in the degraded forested wetland soil cannot fully be identified in the scope of this study, results suggest that abiotic processes dominate the $CHCl_3$ formation at the field sites

4.1.4. Environmental Controls on $CHCl_3$ Emissions. Temperature is well-known to control $CHCl_3$ formation rates in soils and water. In a seasonal measurement of $CHCl_3$ from arctic and subarctic ecosystems, highest fluxes were observed in summer.[49] Indeed, fluxes from laboratory soil core incubations showed a positive correlation with incubation temperatures and could be adequately described by linear Arrhenius equations (R^2 = 0.96, Figure 4b, eq 2). Nevertheless, as shown in Figure 2a,f and Table 1, the $CHCl_3$ emission rates in South Carolina are not correlated with annual temperature fluctuations, suggesting that temperature is not the sole controlling factor of soil $CHCl_3$ emissions at the field site. On the basis of these seemingly contradictory results, we hypothesize, that over the time scale of a year, environmental factors other than temperature (e.g., soil redox potential, chemical precursors advection by high/low tide cycles) dominate the soil $CHCl_3$ production in natural systems. When other geochemical factors are held constant, temperature appears to control the $CHCl_3$ production rate, following the Arrhenius equation.

Hydrological extremes also affect fluxes. For example, the lowest flux (44 ± 7 nmol m^{-2} d^{-1}) was recorded in January when the site was flooded, suggesting that standing water can inhibit $CHCl_3$ emissions by limiting the mass transfer between soil pore air and the ambient air. The highest $CHCl_3$ fluxes were observed from the moist soils in March and December during the transition periods between the flooding and drained conditions. The finding is consistent with the results of fieldwork and laboratory incubations conducted with Alaska Arctic tundra soils,[11,77] which demonstrated that either flooded or drier conditions reduces $CHCl_3$ emissions while saturated (moderate moist) soil without standing water is a common feature for large $CHCl_3$ emissions. This may be related to the fluctuating soil redox potentials as discussed above.

The potential impact of sunlight on halocarbon fluxes is supported by halocarbon emissions following the diurnal cycle of irradiation during measurements in Irish peatlands.[43] However, in the opaque versus transparent chamber measurements, there was no statistically significant difference in $CHCl_3$ fluxes (paired-*t*-test). This suggests that $CHCl_3$ formation in this ecosystem is independent of solar radiation. Results from laboratory incubations of soil cores from Alaska arctic tundra also suggested that formation processes are not necessarily

DOI: 10.1021/acsearthspacechem.8b00044
ACS Earth Space Chem. 2018, 2, 955−967

dependent on sunlight.[11] Thus, it is possible that temperature increases in chambers (varies +15 °C on days with bright sunshine) may account for the previously observed diurnal cycles[43] instead of sunlight. However, it is noted that the photosynthetic active radiation intensity (10−87 μmol m^{-2} s^{-1}) under the canopy of the degraded forested wetland was low, which may hinder the conclusion above that sunlight was not involved in the $CHCl_3$ production.

4.2. Methyl Halides (CH_3Cl and CH_3Br). *4.2.1. Comparison to Fluxes from Other Terrestrial Ecosystems.* In contrast to salt marshes which are significant sources of methyl halides,[79−81] results from this study indicate that the adjacent transitional zone (degraded forested wetland) acts as a net sink for CH_3Cl with an annual mean ± 1σ of −90 ± 61 nmol m^{-2} d^{-1}. As shown in Table 4, the observed net uptake rate of CH_3Cl is on the same order of magnitude but smaller than reported fluxes from tropical rain forest soils,[41] subtropical coastal/chaparral shrublands,[78] temperate passure and grassland,[45] boreal forest soils,[40] and Arctic nonflooded tundra[37] and larger than fluxes from Arctic Greenland mossy soil,[41] temperate wetland,[45] and Arctic flooded tundra.[37]

As for CH_3Br fluxes in our field measurements, they fluctuated between slightly positive and slightly negative values in the range of −6 nmol m^{-2} d^{-1} to 4 nmol m^{-2} d^{-1}, which were negligible.

4.2.2. CH_3Cl and CH_3Br Consumption and Production Mechanisms. The thermal treatment (150 °C for 2 h) switched the soil cores from net sinks to sources for CH_3Cl and CH_3Br. This high temperature should deactivate the microbial and enzymatic activities;[82] therefore, the switch from sink to source suggests that the consumption of methyl halides within the soil was biotic and the production was abiotic predominantly. The finding is further supported by other studies.[36,40,83,84] Biotic consumption exceeded abiotic production, thus yielding net sinks, similar to other soils where gross fluxes were measured.[37,40,84] An abiotic production mechanism[15,85] for methyl halides entails the alkylation of halide ions during the oxidation of organic matter by an electron acceptor such as Fe(III) even in the absence of sunlight or microbial activity. This mechanism may be linked to the $CHCl_3$ production described above. Indeed, the correlation between net $CHCl_3$ emissions and the abiotic production of CH_3Cl from the thermally treated soil cores is strong (R^2 = 0.928, Figure 4d,e).

However, the high CH_3Cl and CH_3Br productions within the saltmarsh are likely created by enzymatic processes in saltmarsh plants, which involves SAM (S-adenosyl-methionine)-dependent methyl transferases that are found widely in plants.[17,21−25]

4.2.3. Environmental Controls on CH_3Cl Emissions. A dependence of methyl halide formation on solar irradiation was proposed previously.[86,87] However, there is no statistically significant difference between the CH_3Cl fluxes measured with opaque and transparent chambers (paired-*t*-test), suggesting that sunlight was not required for either degradation or abiotic production of CH_3Cl. The abiotic production of methyl halides through the oxidation of organic matter by iron(III) is not dependent on sunlight.[15] On the other hand, the photosynthetic active radiation intensity (10−87 μmol m^{-2} s^{-1}) on the ground of the degraded forested wetland where chambers were placed is low, which may mitigate the conclusion above that sunlight was not involved in the production or degradation of CH_3Cl. Therefore, further experiments in more light-exposed environments (e.g., advanced degraded forests with more open canopies) should be conducted to test the light effect.

The post-thermal treated soil incubations demonstrated that the abiotic production of CH_3Cl was temperature controlled, and could be described by Arrhenius equations (Figure 4d, eq 2).

Over the course of the year, neither the highest nor the lowest CH_3Cl fluxes were observed during the flooding season in January and the dry period in July. However, large CH_3Cl uptake rates were observed in May and December during the middle of flooding-drainage cycles when comparably moderate soil moisture was recorded, suggesting that the consumption of CH_3Cl is maximum at intermediate soil moisture and reduced at both low and high ends of the range.[88]

4.3. Regional and Global Implications. Because of the large variability of observed $CHCl_3$ and CH_3Cl fluxes, the heterogeneity of soils and the limited scale of the flux chamber coverage area, any extrapolations to the global scale will introduce large uncertainties. However, a simple quantitative extrapolation can help us to assess the significance of degraded forested tidal wetland in terms of regional halocarbon budgets.

Assuming the annually averaged fluxes of $CHCl_3$ (146 ± 129 nmol m^{-2} d^{-1}) and CH_3Cl (−90 ± 61 nmol m^{-2} d^{-1}) are representative of coastal degraded forested wetland, and using the degraded forested wetland area of 1.7×10^{11} m^2 (including the coastal freshwater wetland subject to seawater inundation) for the continental United States,[89] we estimate a total annual flux of 1.06 ± 0.15 Gg $CHCl_3$ and −0.46 ± 0.05 Gg CH_3Cl. Considering sea level rise and increasing frequency of extreme weather events due to global climate change,[90] the investigated environments thus may become a more important source of ozone-depleting $CHCl_3$. If an annual flux of 270 Gg is needed to balance the OH sink for $CHCl_3$,[91] the coastal forested wetland within the continental United States accounts for 0.4% of the global annual $CHCl_3$ flux, which is not that significant. The uptake of CH_3Cl within the continental United States is also minor compared to the global scale sources and sinks. However, the contributions of global coastal freshwater wetland to halocarbon budgets are expected to be much higher. Unfortunately, the global coastal forested wetland subject to seawater intrusion area data are not currently available.[92] Over longer time scales with sea level rise, the transitional zone is likely to shift further inland and the original degraded forested wetland would convert to saltmarsh. Hence, it is conceivable that the current CH_3Cl sink will become a CH_3Cl source (258 nmol m^{-2} d^{-1} as in May 2012), and instead of an annual uptake of 0.46 Gg CH_3Cl, the area that is currently degraded forested wetland could produce 1.79 Gg of CH_3Cl per year. A longer-term network of measurements across the southeastern US will provide a more accurate assessment of the impact of degraded forested wetlands on ozone-depleting compound budgets at the regional or global scale.

5. CONCLUSIONS

Results from this study suggest that when freshwater forest becomes degraded through seawater intrusion due to storm surges and sea level rise, it emits significant amounts of $CHCl_3$ through abiotic pathways and absorbs CH_3Cl through biotic pathways, and if these lands are overtaken by salt marshes, methyl halide emissions, instead of consumptions, will likely increase. Thus, global warming induced sea level rise could

DOI: 10.1021/acsearthspacechem.8b00044
ACS Earth Space Chem. 2018, 2, 955−967

lead to a potential impact on stratospheric ozone depletion by altering the atmospheric halocarbon budgets. However, it is not yet proven that emissions will dramatically differ from freshwater wetlands, owing to the large spatial and temporal variability of observed fluxes and the limited number of freshwater wetland measurements. Variations could be even larger under different climate conditions (i.e., hurricane, a wet year with more precipitation, etc.).

AUTHOR INFORMATION

Corresponding Author

*Phone: (+1) 510-643-6984. E-mail: jiaoyi@berkeley.edu.

ORCID

Yi Jiao: 0000-0001-5027-3144

Alex T. Chow: 0000-0001-7441-8934

Present Addresses

[§]A.R.: Department of Biogeochemical Processes, Max Planck Institute for Biogeochemistry, 07745, Jena, Germany

[∥]M.J.D.: Department of Soil, Water, and Climate, University of Minnesota—Twin Cities, St. Paul, Minnesota 55108, United States

Notes

The authors declare no competing financial interest.

ACKNOWLEDGMENTS

The authors would like to thank the Natural Science Foundation (grants EAR-1529927 and EAR-1530375) for financial support. The authors are also grateful to Samuel Lin, Wenchen Liu for assistance on the access to the field, Jun-Jian Wang, Dennis Zellmann, David Miller and Hunter Robinson for the assistance on fieldwork, and Jerrold Acdan, Rory French, Bernard Koh, Anya Mikheicheva and Connor Shingai for assistance on laboratory analysis. The manuscript is greatly improved by incorporating the constructive comments and suggestions from three anonymous reviewers, who are hereby warmly appreciated. This work is technical contribution No. 6699 of the Clemson University Experiment Station.

REFERENCES

(1) Elkins, J. W.; Thompson, T. M.; Swanson, T. H.; Butler, J. H.; Hall, B. D.; Cummings, S. O.; Fishers, D. A.; Raffo, A. G. Decrease in the growth rates of atmospheric chlorofluorocarbons 11 and 12. *Nature* **1993**, *364* (6440), 780−783.

(2) Velders, G. J. M.; Andersen, S. O.; Daniel, J. S.; Fahey, D. W.; McFarland, M. The importance of the Montreal Protocol in protecting climate. *Proc. Natl. Acad. Sci. U. S. A.* **2007**, *104* (12), 4814−4819.

(3) Carpenter, L. J.; Reimann, S.; Engel, A.; Montzka, S.; Burkholder, J. B.; Clerbaux, C.; Hall, B.; Yvon-Lewis, S. A.; Blake, D. R.; Dorf, M.; et al.. Update on ozone-depleting substances (ODSs) and other gases of interest to the Montreal Protocol, Chapter 1. *Scientific Assessment of Ozone Depletion: 2014*; Global Ozone Research and Monitoring Project; WMO, 2014; p 416. (Page 1.29 and 1.39).

(4) Mead, M. I.; White, I. R.; Nickless, G.; Wang, K.-Y.; Shallcross, D. E. An estimation of the global emission of methyl bromide from rapeseed (*Brassica napus*) from 1961 to 2003. *Atmos. Environ.* **2008**, *42* (2), 337−345.

(5) Rudolph, J.; Khedim, A.; Koppmann, R.; Bonsang, B. Field study of the emissions of methyl chloride and other halocarbons from biomass burning in western Africa. *J. Atmos. Chem.* **1995**, *22* (1−2), 67−80.

(6) Ferek, R. J.; Reid, J. S.; Hobbs, P. V.; Blake, D. R.; Liousse, C. Emission factors of hydrocarbons, halocarbons, trace gases and particles from biomass burning in Brazil. *J. Geophys. Res. Atmospheres* **1998**, *103* (D24), 32107−32118.

(7) Yokouchi, Y.; Nojiri, Y.; Barrie, L. A.; Toom-Sauntry, D.; Fujinuma, Y. Atmospheric methyl iodide: high correlation with surface seawater temperature and its implications on the sea-to-air flux. *J. Geophys. Res. Atmospheres* **2001**, *106* (D12), 12661−12668.

(8) Smythe-Wright, D.; Boswell, S. M.; Breithaupt, P.; Davidson, R. D.; Dimmer, C. H.; Eiras Diaz, L. B. Methyl iodide production in the ocean: implications for climate change. *Glob. Biogeochem. Cycles* **2006**, *20* (3), GB3003.

(9) Wang, J.-J.; Jiao, Y.; Rhew, R. C.; Chow, A. T. Haloform formation in coastal wetlands along a salinity gradient at South Carolina, United States. *Environ. Chem.* **2016**, *13* (4), 745−756.

(10) Clerbaux, C.; Cunnold, D. M.; Anderson, J.; Engel, A.; Fraser, P. J.; Mahieu, E.; Manning, A.; Miller, J.; Montzka, S. A.; Nassar, R.; et al. Scientific Assessment of Ozone Depletion: 2006. *Glob. Ozone Res. Monit. Proj.− Rep.* **2007**, *50*, 1.15.

(11) Rhew, R. C.; Teh, Y. A.; Abel, T.; Atwood, A.; Mazéas, O. Chloroform emissions from the Alaskan Arctic tundra. *Geophys. Res. Lett.* **2008**, *35* (21), L21811.

(12) Butler, J. H. Atmospheric chemistry: better budgets for methyl halides? *Nature* **2000**, *403* (6767), 260−261.

(13) Cox, M. L.; Sturrock, G. A.; Fraser, P. J.; Siems, S. T.; Krummel, P. B.; O'Doherty, S. Regional sources of methyl chloride, chloroform and dichloromethane identified from AGAGE observations at Cape Grim, Tasmania, 1998−2000. *J. Atmos. Chem.* **2003**, *45* (1), 79−99.

(14) Keene, W. C.; Khalil, M. A. K.; Erickson, D. J., III; McCulloch, A.; Graedel, T. E.; Lobert, J. M.; Aucott, M. L.; Gong, S. L.; Harper, D. B.; Kleiman, G.; et al. Composite global emissions of reactive chlorine from anthropogenic and natural sources: reactive chlorine emissions inventory. *J. Geophys. Res. Atmospheres* **1999**, *104* (D7), 8429−8440.

(15) Keppler, F.; Eiden, R.; Niedan, V.; Pracht, J.; Schöler, H. F. Halocarbons produced by natural oxidation processes during degradation of organic matter. *Nature* **2000**, *403* (6767), 298−301.

(16) Hamilton, J. T. G.; McRoberts, W. C.; Keppler, F.; Kalin, R. M.; Harper, D. B. Chloride methylation by plant pectin: an efficient environmentally significant process. *Science* **2003**, *301* (5630), 206−209.

(17) Rhew, R. C.; Østergaard, L.; Saltzman, E. S.; Yanofsky, M. F. Genetic control of methyl halide production in *Arabidopsis*. *Curr. Biol.* **2003**, *13* (20), 1809−1813.

(18) Huber, S. G.; Kotte, K.; Schöler, H. F.; Williams, J. Natural abiotic formation of trihalomethanes in soil: results from laboratory studies and field samples. *Environ. Sci. Technol.* **2009**, *43* (13), 4934−4939.

(19) Leri, A. C.; Mayer, L. M.; Thornton, K. R.; Northrup, P. A.; Dunigan, M. R.; Ness, K. J.; Gellis, A. B. A marine sink for chlorine in natural organic matter. *Nat. Geosci.* **2015**, *8* (8), 620−624.

(20) Hoekstra, E. J.; de Leer, E. W. B.; Brinkman, U. A. T. Natural formation of chloroform and brominated trihalomethanes in soil. *Environ. Sci. Technol.* **1998**, *32* (23), 3724−3729.

(21) Wuosmaa, A. M.; Hager, L. P. Methyl Chloride Transferase: A carbocation route for biosynthesis of halometabolites. *Science* **1990**, *249* (4965), 160−162.

(22) Attieh, J. M.; Hanson, A. D.; Saini, H. S. Purification and characterization of a novel methyltransferase responsible for biosynthesis of halomethanes and methanethiol in *Brassica oleracea*. *J. Biol. Chem.* **1995**, *270* (16), 9250−9257.

(23) Saini, H. S.; Attieh, J. M.; Hanson, A. D. Biosynthesis of halomethanes and methanethiol by higher plants via a novel methyltransferase reaction. *Plant, Cell Environ.* **1995**, *18* (9), 1027−1033.

(24) Ni, X.; Hager, L. P. cDNA cloning of *Batis maritima* methyl chloride transferase and purification of the enzyme. *Proc. Natl. Acad. Sci. U. S. A.* **1998**, *95* (22), 12866−12871.

DOI: 10.1021/acsearthspacechem.8b00044
ACS Earth Space Chem. 2018, 2, 955−967

(25) Ni, X.; Hager, L. P. Expression of *Batis maritima* methyl chloride transferase in *Escherichia coli*. *Proc. Natl. Acad. Sci. U. S. A.* **1999**, *96* (7), 3611−3615.
(26) Gan, J.; Yates, S. R.; Ohr, H. D.; Sims, J. J. Production of methyl bromide by terrestrial higher plants. *Geophys. Res. Lett.* **1998**, *25* (19), 3595−3598.
(27) Yokouchi, Y.; Noijiri, Y.; Barrie, L. A.; Toom-Sauntry, D.; Machida, T.; Inuzuka, Y.; Akimoto, H.; Li, H.-J.; Fujinuma, Y.; Aoki, S. A strong source of methyl chloride to the atmosphere from tropical coastal land. *Nature* **2000**, *403* (6767), 295−298.
(28) Rhew, R. C.; Miller, B. R.; Bill, M.; Goldstein, A. H.; Weiss, R. F. Environmental and biological controls on methyl halide emissions from southern California coastal salt marshes. *Biogeochemistry* **2002**, *60* (2), 141−161.
(29) Doyle, T. W.; O'Neil, C. P.; Melder, M. P. V.; From, A. S.; Palta, M. M. Tidal freshwater swamps of the southeastern United States: effects of land use, hurricanes, sea-level rise, and climate change. *Ecology of tidal freshwater forested wetlands of the southeastern United States*; Springer: Dordrecht, 2007; pp 1−28.
(30) Cormier, N.; Krauss, K. W.; Conner, W. H. Periodicity in stem growth and litterfall in tidal freshwater forested wetlands: influence of salinity and drought on nitrogen recycling. *Estuaries Coasts* **2013**, *36* (3), 533−546.
(31) Montelius, M.; Svensson, T.; Lourino-Cabana, B.; Thiry, Y.; Bastviken, D. Chlorination and dechlorination rates in a forest soil — a combined modelling and experimental approach. *Sci. Total Environ.* **2016**, *554*−*555* (Supplement C), 203−210.
(32) Zlamal, J. E.; Raab, T. K.; Little, M.; Edwards, R. A.; Lipson, D. A. Biological chlorine cycling in the Arctic coastal plain. *Biogeochemistry* **2017**, *134* (3), 243−260.
(33) Chow, A. T.; Dai, J.; Conner, W. H.; Hitchcock, D. R.; Wang, J.-J. Dissolved organic matter and nutrient dynamics of a coastal freshwater forested wetland in Winyah Bay, South Carolina. *Biogeochemistry* **2013**, *112* (1−3), 571−587.
(34) Busbee, W. S.; Conner, W. H.; Allen, D. M.; Lanham, J. D. Composition and aboveground productivity of three seasonally flooded depressional forested wetlands in coastal South Carolina. *Southeast. Nat.* **2003**, *2* (3), 335−346.
(35) Krauss, K. W.; Duberstein, J. A.; Doyle, T. W.; Conner, W. H.; Day, R. H.; Inabinette, L. W.; Whitbeck, J. L. Site condition, structure, and growth of baldcypress along tidal/non-tidal salinity gradients. *Wetlands* **2009**, *29* (2), 505−519.
(36) Rhew, R. C.; Chen, C.; Teh, Y. A.; Baldocchi, D. Gross fluxes of methyl chloride and methyl bromide in a California oak-savanna woodland. *Atmos. Environ.* **2010**, *44* (16), 2054−2061.
(37) Rhew, R. C.; Teh, Y. A.; Abel, T. Methyl halide and methane fluxes in the northern Alaskan coastal tundra. *J. Geophys. Res.* **2007**, *112* (G2), G02009.
(38) Emmerich, M.; Bhansali, A.; Lösekann-Behrens, T.; Schröder, C.; Kappler, A.; Behrens, S. Abundance, distribution, and activity of Fe(II)-oxidizing and Fe(III)-reducing microorganisms in hypersaline sediments of Lake Kasin, southern Russia. *Appl. Environ. Microbiol.* **2012**, *78* (12), 4386−4399.
(39) Ruecker, A.; Weigold, P.; Behrens, S.; Jochmann, M.; Laaks, J.; Kappler, A. predominance of biotic over abiotic formation of halogenated hydrocarbons in hypersaline sediments in western Australia. *Environ. Sci. Technol.* **2014**, *48* (16), 9170−9178.
(40) Rhew, R. C.; Aydin, M.; Saltzman, E. S. Measuring terrestrial fluxes of methyl chloride and methyl bromide using a stable isotope tracer technique. *Geophys. Res. Lett.* **2003**, *30* (21), 2103.
(41) Khalil, M. A. K.; Rasmussen, R. A. Soil-atmosphere exchange of radiatively and chemically active gases. *Environ. Sci. Pollut. Res.* **2000**, *7* (2), 79−82.
(42) Rhew, R. C.; Miller, B. R.; Weiss, R. F. Chloroform, carbon tetrachloride and methyl chloroform fluxes in southern California ecosystems. *Atmos. Environ.* **2008**, *42* (30), 7135−7140.
(43) Dimmer, C. H.; Simmonds, P. G.; Nickless, G.; Bassford, M. R. Biogenic fluxes of halomethanes from Irish peatland ecosystems. *Atmos. Environ.* **2001**, *35* (2), 321−330.
(44) Albers, C. N.; Jacobsen, O. S.; Flores, É. M. M.; Pereira, J. S. F.; Laier, T. Spatial variation in natural formation of chloroform in the soils of four coniferous forests. *Biogeochemistry* **2011**, *103* (1−3), 317−334.
(45) Cox, M. L.; Fraser, P. J.; Sturrock, G. A.; Siems, S. T.; Porter, L. W. Terrestrial sources and sinks of halomethanes near Cape Grim, Tasmania. *Atmos. Environ.* **2004**, *38* (23), 3839−3852.
(46) Khalil, M. A. K.; Rasmussen, R. A.; Shearer, M. J.; Chen, Z.-L.; Yao, H.; Yang, J. Emissions of methane, nitrous oxide, and other trace gases from rice fields in China. *J. Geophys. Res. Atmospheres* **1998**, *103* (D19), 25241−25250.
(47) Khan, M. A. H.; Rhew, R. C.; Whelan, M. E.; Zhou, K.; Deverel, S. J. Methyl halide and chloroform emissions from a subsiding Sacramento−San Joaquin Delta island converted to rice fields. *Atmos. Environ.* **2011**, *45* (4), 977−985.
(48) Hellén, H.; Hakola, H.; Pystynen, K.-H.; Rinne, J.; Haapanala, S. C_2-C_{10} hydrocarbon emissions from a boreal wetland and forest floor. *Biogeosciences* **2006**, *3* (2), 167−174.
(49) Johnsen, A. R.; Jacobsen, O. S.; Gudmundsson, L.; Albers, C. N. Chloroform emissions from Arctic and subarctic ecosystems in Greenland and northern Scandinavia. *Biogeochemistry* **2016**, *130* (1−2), 53−65.
(50) Pickering, L.; Black, T. A.; Gilbert, C.; Jeronimo, M.; Nesic, Z.; Pilz, J.; Svensson, T.; Öberg, G. Portable chamber system for measuring chloroform fluxes from terrestrial environments − methodological challenges. *Environ. Sci. Technol.* **2013**, *47* (24), 14298−14305.
(51) Khan, M. a. H.; Whelan, M. E.; Rhew, R. C. Effects of temperature and soil moisture on methyl halide and chloroform fluxes from drained peatland pasture soils. *J. Environ. Monit.* **2012**, *14* (1), 241−249.
(52) Brown, F. S.; Hager, L. P. Chloroperoxidase. IV. Evidence for an ionic electrophilic substitution mechanism. *J. Am. Chem. Soc.* **1967**, *89* (3), 719−720.
(53) Walter, B.; Ballschmiter, K. Formation of C1/C2-bromo-/chloro-hydrocarbons by haloperoxidase reactions. *Fresenius' J. Anal. Chem.* **1992**, *342* (10), 827−833.
(54) Neumann, C. S.; Fujimori, D. G.; Walsh, C. T. Halogenation strategies in natural product biosynthesis. *Chem. Biol.* **2008**, *15* (2), 99−109.
(55) Wagner, C.; El Omari, M.; König, G. M. Biohalogenation: nature's way to synthesize halogenated metabolites. *J. Nat. Prod.* **2009**, *72* (3), 540−553.
(56) Weigold, P.; El-Hadidi, M.; Ruecker, A.; Huson, D. H.; Scholten, T.; Jochmann, M.; Kappler, A.; Behrens, S. A metagenomic-based survey of microbial (de)halogenation potential in a German forest soil. *Sci. Rep.* **2016**, *6*, srep28958.
(57) Hoekstra, E. J.; Lassen, P.; van Leeuwen, J. G. E.; de Leer, E. W. B.; Carlsen, L. Formation of organic chlorine compounds of low molecular weight in the chloroperoxidase-mediated reaction between chloride and humic material. *Environ. Chem.* **1995**, *1*, 149.
(58) Hoekstra, E. J.; Duyzer, J. H.; de Leer, E. W. B.; Brinkman, U. A. T. Chloroform − concentration gradients in soil air and atmospheric air, and emission fluxes from soil. *Atmos. Environ.* **2001**, *35* (1), 61−70.
(59) Pickard, M. A.; Hashimoto, A. Stability and carbohydrate composition of chloroperoxidase from *Caldariomyces fumago* grown in a fructose−salts medium. *Can. J. Microbiol.* **1988**, *34* (8), 998−1002.
(60) Liu, J.-Z.; Wang, M. Improvement of activity and stability of chloroperoxidase by chemical modification. *BMC Biotechnol.* **2007**, *7*, 23.
(61) Schijndel, J. W. P. M. V.; Barnett, P.; Roelse, J.; Vollenbroek, E. G. M.; Wever, R. The stability and steady-state kinetics of vanadium chloroperoxidase from the fungus *Curvularia inaequalis*. *Eur. J. Biochem.* **1994**, *225* (1), 151−157.
(62) Berns, A. E.; Philipp, H.; Narres, H.-D.; Burauel, P.; Vereecken, H.; Tappe, W. Effect of gamma-sterilization and autoclaving on soil organic matter structure as studied by solid state NMR, UV and Fluorescence Spectroscopy. *Eur. J. Soil Sci.* **2008**, *59* (3), 540−550.

DOI: 10.1021/acsearthspacechem.8b00044
ACS Earth Space Chem. 2018, 2, 955−967

(63) Haselmann, K. F.; Laturnus, F.; Grøn, C. Formation of chloroform in soil: a year-round study at a Danish spruce forest site. *Water, Air, Soil Pollut.* **2002**, *139* (1−4), 35−41.
(64) De Leer, E. W. B.; Damste, J. S. S.; Erkelens, C.; De Galan, L. Identification of intermediates leading to chloroform and C-4 diacids in the chlorination of humic acid. *Environ. Sci. Technol.* **1985**, *19* (6), 512−522.
(65) Frank, H.; Frank, W.; Thiel, D. C1- and C2-halocarbons in soil-air of forests. *Atmos. Environ.* **1989**, *23* (6), 1333−1335.
(66) Matucha, M.; Gryndler, M.; Schröder, P.; Forczek, S. T.; Uhlířová, H.; Fuksová, K.; Rohlenová, J. Chloroacetic acids—degradation intermediates of organic matter in forest soil. *Soil Biol. Biochem.* **2007**, *39* (1), 382−385.
(67) Albers, C. N.; Jacobsen, O. S.; Flores, E. M. M.; Johnsen, A. R. Arctic and subarctic natural soils emit chloroform and brominated analogues by alkaline hydrolysis of trihaloacetyl compounds. *Environ. Sci. Technol.* **2017**, *51* (11), 6131−6138.
(68) Müller, G.; Spassovski, M.; Henschler, D. Trichloroethylene exposure and trichloroethylene metabolites in urine and blood. *Arch. Toxicol.* **1972**, *29* (4), 335−340.
(69) Frank, H. Airborne chlorocarbons, photooxidants, and forest decline. *Ambio* **1991**, *20* (1), 13−18.
(70) Haselmann, K. F.; Laturnus, F.; Svensmark, B.; Grøn, C. Formation of chloroform in spruce forest soil − results from laboratory incubation studies. *Chemosphere* **2000**, *41* (11), 1769−1774.
(71) Devlin, J. F.; Müller, D. Field and laboratory studies of carbon tetrachloride transformation in a sandy aquifer under sulfate reducing conditions. *Environ. Sci. Technol.* **1999**, *33* (7), 1021−1027.
(72) McCormick, M. L.; Bouwer, E. J.; Adriaens, P. Carbon tetrachloride transformation in a model iron-reducing culture: relative kinetics of biotic and abiotic reactions. *Environ. Sci. Technol.* **2002**, *36* (3), 403−410.
(73) Laturnus, F.; Fahimi, I.; Gryndler, M.; Hartmann, A.; Heal, M.; Matucha, M.; Schöler, H. F.; Schroll, R.; Svensson, T. Natural formation and degradation of chloroacetic acids and volatile organochlorines in forest soil. challenges to understanding. *Environ. Sci. Pollut. Res.* **2005**, *12* (4), 233−244.
(74) Breider, F.; Hunkeler, D. Mechanistic insights into the formation of chloroform from natural organic matter using stable carbon isotope analysis. *Geochim. Cosmochim. Acta* **2014**, *125* (Supplement C), 85−95.
(75) Breider, F.; Albers, C. N. Formation mechanisms of trichloromethyl-containing compounds in the terrestrial environment: a critical review. *Chemosphere* **2015**, *119* (Supplement C), 145−154.
(76) Page, S. E.; Sander, M.; Arnold, W. A.; McNeill, K. Hydroxyl radical formation upon oxidation of reduced humic acids by oxygen in the dark. *Environ. Sci. Technol.* **2012**, *46* (3), 1590−1597.
(77) Teh, Y. A.; Mazéas, O.; Atwood, A. R.; Abel, T.; Rhew, R. C. Hydrologic regulation of gross methyl chloride and methyl bromide uptake from Alaskan Arctic tundra. *Glob. Change Biol.* **2009**, *15* (2), 330−345.
(78) Rhew, R. C.; Miller, B. R.; Vollmer, M. K.; Weiss, R. F. Shrubland fluxes of methyl bromide and methyl chloride. *J. Geophys. Res. Atmospheres* **2001**, *106* (D18), 20875−20882.
(79) Rhew, R. C.; Miller, B. R.; Weiss, R. F. Natural methyl bromide and methyl chloride emissions from coastal salt marshes. *Nature* **2000**, *403* (6767), 292−295.
(80) Drewer, J.; Heal, M. R.; Heal, K. V.; Smith, K. A. Temporal and spatial variation in methyl bromide flux from a salt marsh. *Geophys. Res. Lett.* **2006**, *33* (16), L16808.
(81) Manley, S. L.; Wang, N.-Y.; Walser, M. L.; Cicerone, R. J. Coastal salt marshes as global methyl halide sources from determinations of intrinsic production by marsh plants. *Glob. Biogeochem. Cycles* **2006**, *20* (3), GB3015.
(82) Hines, M. E.; Crill, P. M.; Varner, R. K.; Talbot, R. W.; Shorter, J. H.; Kolb, C. E.; Harriss, R. C. Rapid consumption of low concentrations of methyl bromide by soil bacteria. *Appl. Environ. Microbiol.* **1998**, *64* (5), 1864−1870.
(83) Rhew, R. C.; Abel, T. Measuring simultaneous production and consumption fluxes of methyl chloride and methyl bromide in annual temperate grasslands. *Environ. Sci. Technol.* **2007**, *41* (22), 7837−7843.
(84) Teh, Y. A.; Rhew, R. C.; Atwood, A.; Abel, T. Water, temperature, and vegetation regulation of methyl chloride and methyl bromide fluxes from a shortgrass steppe ecosystem. *Glob. Change Biol.* **2008**, *14* (1), 77−91.
(85) Keppler, F.; Borchers, R.; Elsner, P.; Fahimi, I.; Pracht, J.; Schöler, H. F. Formation of volatile iodinated alkanes in soil: results from laboratory studies. *Chemosphere* **2003**, *52* (2), 477−483.
(86) Amiro, B. D.; Johnston, F. L. Volatilization of iodine from vegetation. *Atmos. Environ.* **1989**, *23* (3), 533−538.
(87) Muramatsu, Y.; Yoshida, S. Volatilization of methyl iodide from the soil-plant system. *Atmos. Environ.* **1995**, *29* (1), 21−25.
(88) Rhew, R.; Mazéas, O. Gross production exceeds gross consumption of methyl halides in northern California salt marshes. *Geophys. Res. Lett.* **2010**, *37* (18), L18813.
(89) Dahl, T. E.; Stedman, S. M. *Status and trends of wetlands in the coastal watersheds of the conterminous United States 2004 to 2009*; National Oceanic and Atmospheric Administration, National Marine Fisheries Service: Silver Spring, MD, 2013. See the following: https://www.fws.gov/wetlands/Documents/Status-and-Trends-of-Wetlands-In-the-Coastal-Watersheds-of-the-Conterminous-US-2004-to-2009.pdf
(90) Tebaldi, C.; Strauss, B. H.; Zervas, C. E. Modelling sea level rise impacts on storm surges along US coasts. *Environ. Res. Lett.* **2012**, *7* (1), 014032.
(91) O'Doherty, S.; Simmonds, P. G.; Cunnold, D. M.; Wang, H. J.; Sturrock, G. A.; Fraser, P. J.; Ryall, D.; Derwent, R. G.; Weiss, R. F.; Salameh, P.; et al. In situ chloroform measurements at advanced global atmospheric gases experiment atmospheric research stations from 1994 to 1998. *J. Geophys. Res. Atmospheres* **2001**, *106* (D17), 20429−20444.
(92) Herbert, E. R.; Boon, P.; Burgin, A. J.; Neubauer, S. C.; Franklin, R. B.; Ardón, M.; Hopfensperger, K. N.; Lamers, L. P. M.; Gell, P. A global perspective on wetland salinization: ecological consequences of a growing threat to freshwater wetlands. *Ecosphere* **2015**, *6* 10, DOI: 10.1890/ES14-00534.1.

DOI: 10.1021/acsearthspacechem.8b00044
ACS Earth Space Chem. 2018, 2, 955−967